JOURNAL OF PROPULSION AND POWER
Vol. 10, No. 1, Jan.–Feb. 1994

Experimental Investigation of a Supersonic Swept Ramp Injector Using Laser-Induced Iodine Fluorescence

Roy J. Hartfield Jr.,* Steven D. Hollo,† and James C. McDaniel‡
University of Virginia, Charlottesville, Virginia 22903

Nonintrusive optical diagnostic techniques have been employed in an experimental investigation of a supersonic mixing flowfield configured with near-parallel underexpanded injection from the base of a swept ramp. The flowfield has been investigated using both Mach 2 and 2.9 freestreams. Laser-induced iodine fluorescence has been used to conduct planar measurements of the injectant mole fraction distribution in the symmetry plane of the ramp and in crossflow planes. The measurements dramatically illustrate the domination of the mixing process by streamwise vorticity generated by the ramp. The vortices bring freestream air into the center of the plume and lift the plume away from the injection wall. A transition from a vortex-dominated mixing region to a region in which mixing is dominated by turbulence is observed at approximately 10 ramp heights downstream of the injector. No significant shock-induced effects on the mixing process are noted in the near field of the injector. Additionally, the mixing rate is observed to be lower for Mach 2.9 freestream than for Mach 2 freestream. These measurements provide both fundamental insight into the vortex-enhanced mixing process and an accurate and extensive experimental data base for the validation of computational fluid dynamic codes developed for the calculation of highly three-dimensional supersonic mixing flowfields.

Introduction

VORTEX-ENHANCED mixing, often referred to as hypermixing, involves the use of streamwise vortices to mix two streams. Reference 1 contains a review of investigations of vortex-enhanced mixing in which both subsonic and supersonic injectors are exhausted into static and subsonic freestreams. The subject of this investigation is the experimental characterization of the mixing of a proposed scramjet injector design which relies heavily on large-scale streamwise vorticity in the supersonic primary stream to mix injectant from a near-parallel injector. The motivation for this design is to maintain high mixing efficiencies with a minimum total pressure loss for high combustor Mach numbers. The combustor test section configuration is a swept ramp centered on one wall of a constant-height rectangular duct with a circular injector located in the rectangular base of the ramp. A drawing of the swept ramp injector model is presented in Fig. 1. The reacting version of this flowfield has also been investigated both experimentally[2] and numerically.[3,4]

The measurements presented herein were conducted in nonreacting combustor test sections with air injection into air. In this injector geometry, large scale streamwise vortices are generated by freestream air spilling around the ramp. These vortices dramatically influence the mixing of the injectant with the freestream air. The strength, structure, and influence of the vortices can vary significantly with combustor inlet Mach number. Since the SCRAMJET combustor is expected to operate over a range of Mach numbers, it is important to experimentally investigate the effect of inlet Mach number on the injectant mole fraction distribution. In this work, injectant mole fraction distributions across the combustor test section were measured at 15 locations for Mach 2 and 2.9 inlet conditions. The mixing efficiency is evaluated based on two different mixing definitions and plotted as a function of duct length for the two inlet Mach numbers.

Flowfield Geometry

The injector ramp angle is 9.5 deg and the ramp side walls are swept at 9.5 deg, as shown in Fig. 1. The ramp is 30 mm along its top face and has a base which is 4.9 mm tall and 7.6 mm wide. The diameter of the injector at its exit is 3.3 mm and it has an area ratio of 1.34, corresponding to an exit Mach number of 1.7. The 30.5-mm-wide test section is a constant-area channel, except for the ramp. The height of the Mach 2 test section is 18.1 mm and the height of the Mach 2.9 test section is 19.3 mm. A schematic diagram of the Mach 2 flowfield is given in Fig. 2. The principle features of the flowfield include the ramp-generated oblique shock and its reflection from the opposite tunnel wall, an expansion fan at

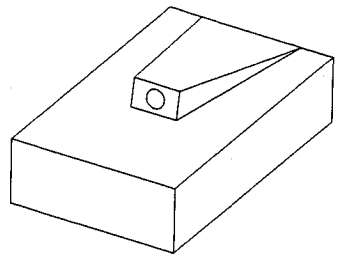

Fig. 1 Swept ramp model.

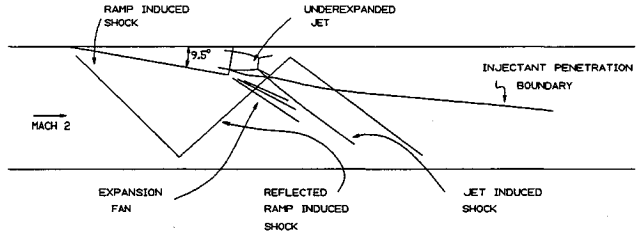

Fig. 2 Swept ramp injector flowfield schematic.

Presented as Paper 90-1518 at the AIAA 21st Fluid Dynamics, Plasma Dynamics and Lasers Conference, Seattle, WA, June 18–20, 1990; received Oct. 23, 1991; revision received Jan. 4, 1993; accepted for publication Feb. 14, 1993.

*Graduate Research Assistant, Department of Mechanical and Aerospace Engineering; currently Assistant Professor of Aerospace Engineering, Auburn University, Auburn, AL 36849. Member AIAA.

†Graduate Research Assistant, Department of Mechanical and Aerospace Engineering; currently Research Scientist. Member AIAA.

‡Associate Professor, Department of Mechanical and Aerospace Engineering. Member AIAA.

the tip of the ramp, a barrel shock, and Mach disc associated with the underexpanded injector and a shock emanating from the Mach disc.

Optical Measurement Techniques

A conventional laser shadowgraph setup, including a microscope objective, a spatial filter, a collimating lens, a screen, and a film camera was used to produce the shadowgraphs presented herein. Planar laser-induced iodine fluorescence (PLIIF) has been used as the primary flow diagnostic in this investigation. PLIIF has been used to visualize mixing flows,[5-7] to measure the thermodynamic variables in compressible flows,[8-11] and to measure injectant mole fractions in compressible mixing flows.[12-14] High signal levels, excellent spatial resolution, and positioning accuracy in three dimensions, and the potential for spatially complete, nonintrusive measurements of flowfield parameters make PLIIF extremely attractive as a flow diagnostic. For the planar mole fraction measurements presented herein, both the spatial resolution and spatial accuracy is estimated to be approximately 200 μm in each direction. For the fluorescence visualization photographs and the injectant mole fraction measurements presented herein, the P13,R15 iodine absorption transitions in the 43-O vibrational band were excited by the 514.5-nm line of the argon ion laser.

The technique for determining injectant mole fraction in compressible mixing flows using laser-induced fluorescence is described in detail in Ref. 12. The fluorescence signal resulting from laser excitation of molecules or atoms seeded into a flowfield is dependent on the thermodynamic state of the flow, the local laser power, and the local concentration of the irradiated seed molecule. For low speed incompressible flows in which the thermodynamic state is constant, the detected fluorescence signal is linearly proportional to the concentration of the seed molecule and the local laser power. However, in compressible flows, the thermodynamic dependence of the fluorescence signal prevents the direct measurement of the seeded species concentration from the measured fluorescence signal. The injectant mole fraction measurement technique eliminates the thermodynamic dependence of the signal by employing a simple ratio of the signal collected with only the injector seeded with iodine to the signal collected with the entire flowfield seeded.[12] For the seeding levels employed in this investigation (10^{-4} parts I_2), the thermodynamic state of the gas is unaffected by the seeding and the thermodynamic dependence of the fluorescence signal at a specified flowfield location is the same for both seeding conditions, provided the stagnation conditions are unaltered by the seeding process. Additionally, if the same laser sheet arrangement is employed for both measurements, the power distribution in the laser sheet is normalized in the signal ratio. Therefore, for nonreacting flowfields, this resulting signal ratio is directly proportional to the ratio of the injectant number density to the total number density, or injectant mole fraction. Because of the reduced flow rate in the mixing vessel with only the injector seeded, the iodine seeding fraction for the injector when only the injector is seeded is generally higher than the seeding fraction when the entire flow is seeded. This makes the signal in the injector plume uniformly larger when only the injector is seeded; therefore, the signal ratio must be multiplied by a constant which is equal to the ratio of the seeding fraction with the entire flow seeded to the seeding fraction with only the injector seeded in order to convert the signal ratio into an accurate representation of the injectant mole fraction distribution. This scaling constant is determined at the exit of the injector where the injectant mole fraction is known to be unity. Using standard uncertainty analysis techniques, the uncertainty of the injectant mole fraction measurement technique, when employed with the optical setup described herein, is estimated to be between 2 and 3%. It should be noted that uncertainties in PLIIF measurements associated with the condensation of the iodine seed species in the cold supersonic flow are addressed in detail in Ref. 13.

The injectant mole fraction measurement approach can be applied directly with no spatial distortion in planes which are parallel or nearly parallel to the tunnel centerline. Direct measurements in crossflow planes are complicated because detectors cannot be placed normal to the crossflow measurement planes. However, the crossflow mole fraction distributions can be determined in two ways. Measurements in many successive planes parallel to the tunnel centerline can be conducted and, using the data in each of those planes, the crossflow mole fraction distributions can be numerically constructed. This approach has been successfully employed and is described in detail in Ref. 14. Alternatively, the detector can be oriented at an angle to the crossflow planes. This leads to some spatial distortion; however, for the experimental setup employed in this investigation, it was determined that the spatial distortion in the vicinity of the injectant plume was minimal (less than 1%). The direct crossflow imaging approach was employed in this investigation because this technique offers the highest accuracy and spatial resolution. The details and merits of this approach are discussed in Ref. 15.

The optical setup for the measurements presented herein consists primarily of an argon ion laser and a liquid-nitrogen-cooled CCD camera system. The argon ion laser (Spectra Physics Model 171) is operated with 6 W output power on the 514.5-nm line. The laser beam is converted into a 200-μm-thick sheet for planar imaging using a 6.8-mm-focal-length cylindrical lens and a 300-mm-focal-length spherical lens. The liquid-nitrogen-cooled CCD camera, chosen for its intrinsic linearity, high quantum efficiency, and low noise characteristics, is a Photometrics CH210 equipped with a PM512 (512 $\times$ 512) CCD. The camera controller, which is connected to a microcomputer, is equipped with a 14-bit image digitizer which takes advantage of most of the 30,000:1 dynamic range of the cooled CCD. The camera and the final turning mirror for the laser sheet are mounted on a single-axis, computer-controlled positioning device to maintain the focus and field of view for all measurement planes. The fluorescence is imaged through a long-pass reflecting filter, a long-pass absorbing filter and a 50-mm-focal-length Nikon f1.8 lens. An Olympus OM2-S film camera was employed for the shadowgraphs and planar fluorescence visualization photographs. For the shadowgraphs, the argon ion laser was the light source. The laser beam was converted into a uniform 15-cm-diam column of light using a microscope objective, a spatial filter and a 570-mm-focal-length spherical lens.

Flowfield Conditions

Measurements at freestream Mach numbers of 2 and 2.9 were obtained using two separate test sections. Both test sections were equipped with fused silica windows on three sides of the duct for excellent optical access. The ratio of injector mass flow rate to tunnel mass flow rate was held constant for the two Mach numbers to simulate the same combustor equivalence ratio. The total pressure for the Mach 2 test section freestream was 262 and 252 kPa for the injector. The total pressure for the Mach 2.9 test section freestream was 517 and 231 kPa for the injector. The resulting ratio of the injector total pressure to freestream static pressure is approximately twice as large for the Mach 2.9 flowfield as that for the Mach 2 flowfield. For this reason, the injector is much more underexpanded at the higher Mach number.

Results and Discussion

Some of the major flowfield characteristics of underexpanded injection behind a swept ramp into a supersonic freestream can be seen in the shadowgraphs displayed in Fig. 3. The shadowgraph shown in Fig. 3a was collected with the injector off and the shadowgraph shown in Fig. 3b was collected with the injector on. The ramp-generated oblique shock is nonplanar. Near the beginning of the ramp, the angle between this shock and the flow direction is 38 deg. Away from

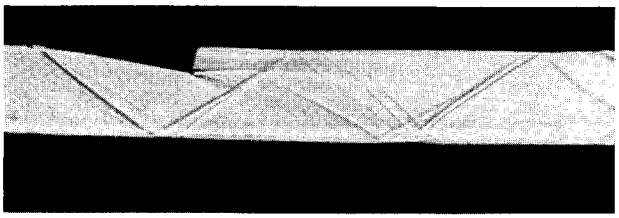

a) Without injection

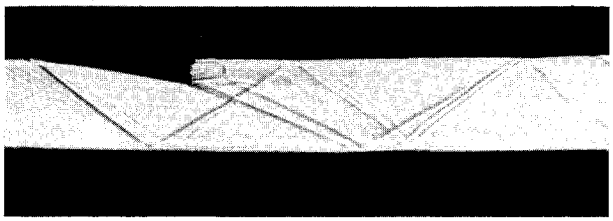

b) With injection

Fig. 3 Shadowgraphs of swept ramp in a Mach 2 freestream.

a) With injector seeded

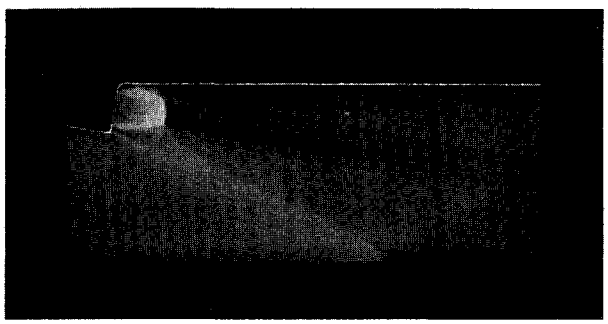

b) With entire flow seeded

Fig. 4 Fluorescence photographs of swept ramp injector in a Mach 2 freestream.

the ramp, near the opposite wall, the angle between this shock and the flow direction approaches 37 deg. These measured angles are slightly less than the 39-deg planar oblique shock angle calculated for Mach 2 flow over a two-dimensional 9.5 deg wedge. A small expansion fan centered on the tip of the ramp and a shear layer having an origin at the tip of the ramp are discernable in Fig. 3a. In Fig. 3b the barrel shock of the underexpanded injector, which is approximately one ramp height in length, and a weak shock system associated with the injector core can be seen. Also discernable in Fig. 3b is the turning of the underexpanded jet barrel shock toward the wall of the injector. It is apparent that, at Mach 2, the ramp-generated shock is reflected into the region immediately downstream of the injector core for this test section geometry.

Photographs of the fluorescence induced at the centerline of the swept ramp test section are shown in Fig. 4. Figure 4a is an image of the fluorescence with only the injector seeded and Fig. 4b is an image of the fluorescence with the entire flowfield seeded. It has been shown that, for uniformly seeded flows, the fluorescence resulting from the excitation of the P13,R15 iodine absorption transitions by a broadband laser is a monotonically decreasing function of temperature for temperatures greater than approximately 10 K.[10] For this reason, in Fig. 4b bright areas represent low-temperature regions of the flow and dark areas represent high-temperature regions. Also, features in which large temperature gradients are present (such as shocks and shear layers) are clearly visible. The increasing fluorescence intensity in the core of the injector is indicative of the decreasing temperature in the expansion. It is apparent that the core of the underexpanded injector is at a much lower temperature than the freestream. The temperature immediately downstream of the clearly defined Mach disk at the end of the barrel shock and in the injector plume is higher than the freestream temperature. Because of this strong temperature dependence of the fluorescence, images of fluorescence with only the injector seeded cannot be used to quantitatively determine injectant concentration or mole fraction directly; however, it is apparent from the planar fluorescence visualization image of Fig. 4a that the injectant plume is lifted away from the injector wall downstream of the injector core, even though the shadowgraphs suggested an initial turning of the injector core toward this wall.

A pseudocolor plot of the injectant mole fraction measurement for the Mach 2 test section in the plane parallel to the test section centerline and centered on the injector is given in Fig. 5. By comparing this plot to the fluorescence visualization photographs, it can be observed that the 100% contour lies near the boundary of the underexpanded core of the injector. Near the wall of the ramp the injectant mole fraction is reduced to less than 10% within approximately two ramp heights of the injector exit. Downstream of this point a layer having a low injectant mole fraction separates the bulk of the injectant plume from the wall. It should be noted that in the near field of the injector, the reflected ramp-generated oblique shock has no apparent effect on mixing; however, a slight, relatively abrupt turn in the bottom plume boundary is discernable at approximately 8 ramp heights downstream of the injector exit. By comparing this mole fraction distribution with the shadowgraphs in Fig. 3 and the fluorescence photograph in Fig. 4b, it is apparent that this turn in the plume boundary occurs in the vicinity of a set of oblique shocks, indicating that shocks do have a measurable influence on the trajectory of the injectant plume, as expected.

Most of the crossflow injectant mole fraction measurement planes do not contain an area of 100% injectant which can be used to determine the scaling constant needed to correct the signal ratios for variations in the seeding fraction, as described earlier. For this reason, the scaling constants for the crossflow images presented herein were obtained in the following way. A centerline injectant mole fraction image, such as the one presented in Fig. 5, was generated first. The injectant mole fraction distribution along the centerline of each crossflow measurement was then matched to the corresponding line of mole fraction data in the tunnel centerline distribution. The measurements of injectant mole fraction in the crossflow planes for the Mach 2 freestream condition are rep-

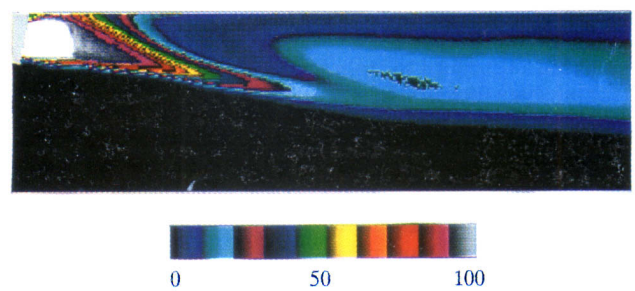

Fig. 5 Centerline mole fraction distribution at Mach 2.

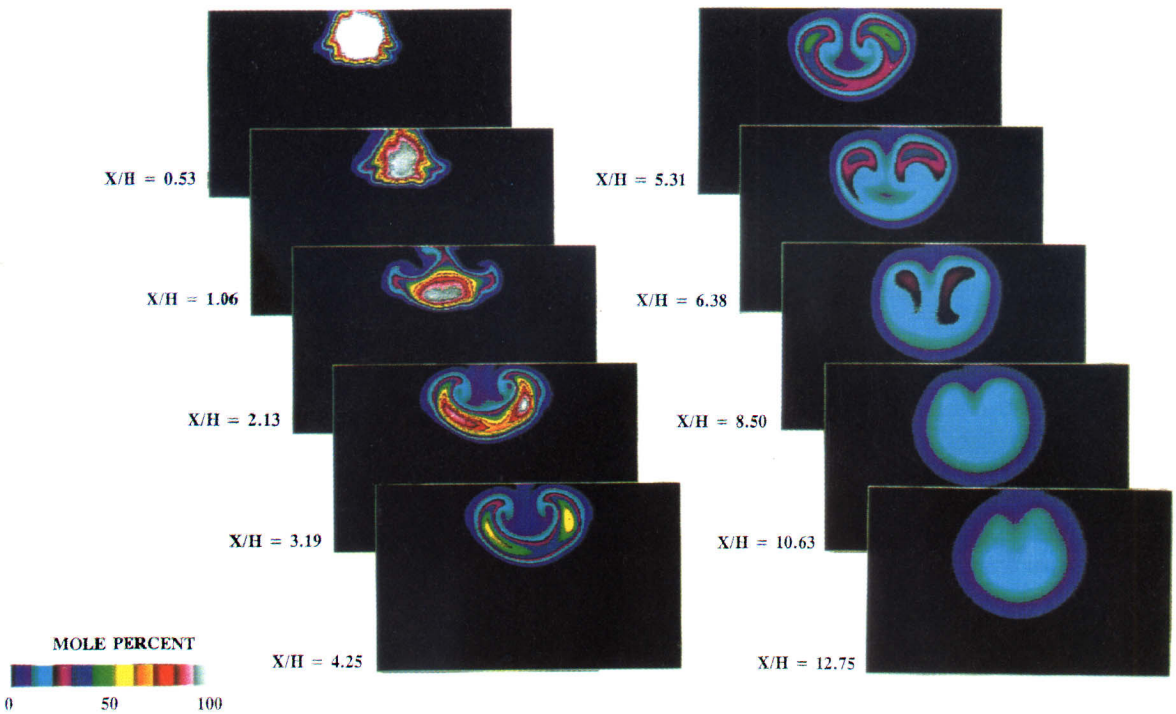

Fig. 6 Crossflow injectant mole fraction distributions from swept ramp injector at Mach 2.

resented in the pseudocolor images in Fig. 6. It is the measurements in these planes that reveal the dominate role of the ramp-generated streamwise vortices in the mixing process. Relevant to the SCRAMJET application is the fact that 30% injectant mole fraction would represent the stoichiometric mixture for hydrogen-air combustion. Included in Fig. 6 are the injectant mole fraction distributions at X/H = 0.53, 1.06, 2.13, 3.19, 4.25, 5.31, 6.38, 8.50, 10.63, and 12.75, where X is the distance downstream of the intersection of the base of the ramp with the injector wall and H is the ramp height. At 0.53 ramp heights, the shape of the injectant plume is dominated by the round core of the underexpanded jet; however, a distinct distortion of the plume fringes by ramp-generated vortices is notable. At 1.06 ramp heights, the core of the plume retains the basic round shape of the injector but the lower mole fraction contours are more seriously affected by the vortex structure generated by the ramp. At 2.13 ramp heights a reduced injector core is still present, but the shape and the lower mole fraction contours are dramatically affected by the vortices and some asymmetry in the plume is noted. (This asymmetry is due to an imperfect nozzle contour.) At this point the entire plume is beginning to separate from the injector wall. At 3.19 ramp heights the core of the injectant plume has virtually disappeared and most of the injectant is in a half-circle band. The vortices have forced freestream air into the center of the plume and completely separated the injectant plume from the injector wall. At 4.25 ramp heights the injectant mole fraction in the central region of the plume has been significantly reduced, but the injectant is still in the half-circle band formed by the vortices. At 5.31 ramp heights the highest injectant mole fraction regions lie toward the tips of the half-circular band. The maximum injectant mole fraction has been reduced to approximately 50% and an increase in the injectant mole fraction in the central region of the plume is observed at this location. At 6.38 ramp heights the injectant mole fraction along the center of the plume is uniformly about 10% and the maximum injectant mole fraction is approximately stoichiometric. At 8.5 ramp heights, the plume is becoming circular with concentration everywhere below stoichiometric. The only remaining influence of the coherent vortex structure on the mixing process is the presence of two separated lobes of 20% injectant and a slight dip in the outer

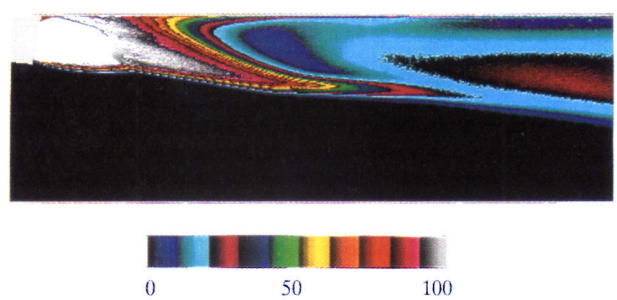

Fig. 7 Centerline mole fraction distribution at Mach 2.9.

plume contour along the top of the plume. The mole fraction distributions at 10.63 ramp heights and 12.75 ramp heights indicate that the dramatic influence of the coherent vortex structure on the injectant plume has been substantially reduced.

Figure 7 is a pseudocolor plot of the injectant mole fraction distribution in the centerline plane of the swept ramp injector flowfield with a freestream Mach number of 2.9. Note that the higher mole fraction contours are generally further downstream than in the Mach 2 flowfield. The 10% injectant contour is completely enclosed and immediately below this low injectant mole fraction cell is a narrow band containing high levels of injectant. In this injectant plume, significant levels of injectant are present in the boundary layer downstream of the injector core and the low injectant mole fraction layer which separates the plume from the injector wall develops much further downstream than at Mach 2.

The pseudocolor plots displayed in Fig. 8 are injectant mole fraction distributions in the Mach 2.9 flowfield. The locations of these distributions are the same as those presented in Fig. 6 for the Mach 2 flowfield. In the distribution at 0.53 ramp heights the injectant plume is dominated by the underexpanded injector core and the injectant contours again take the shape of the round injector exit. At 1.06 ramp heights the lower mole fraction contours are beginning to be affected by the streamwise vorticity. The distribution at 2.13 ramp heights still has some regions of near 100% injectant mole fraction but the shape of the injectant plume is much more

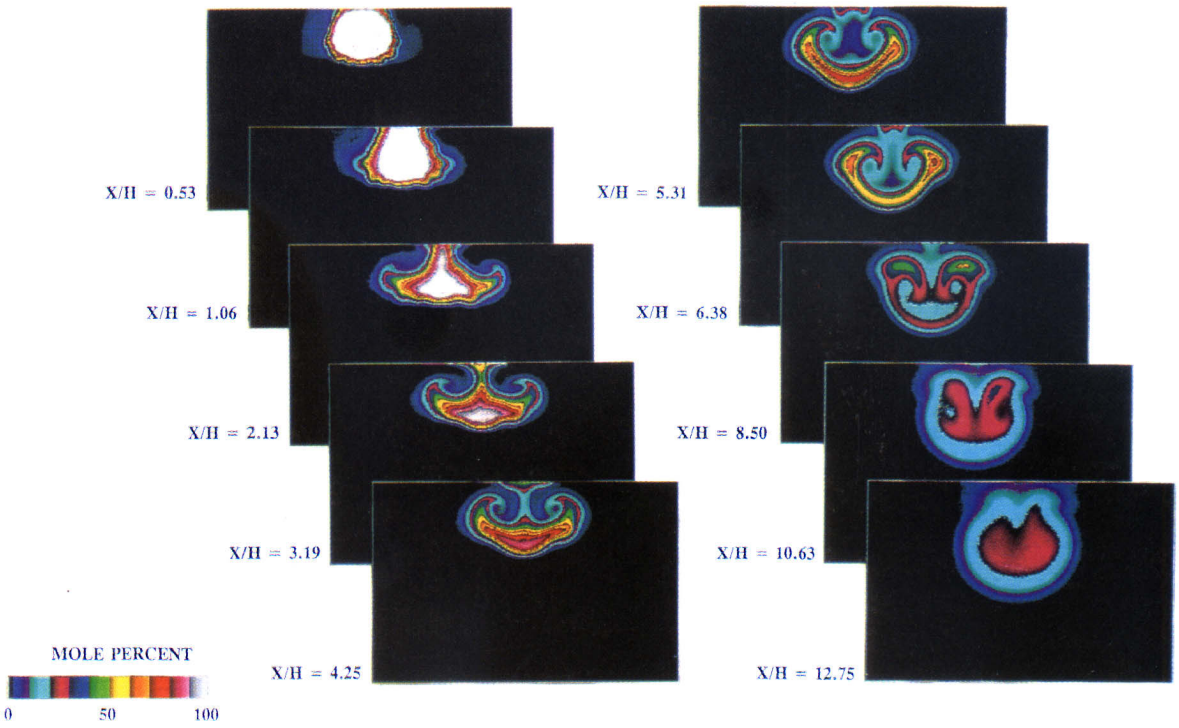

Fig. 8 Crossflow injectant mole fraction distributions from swept ramp injector at Mach 2.9.

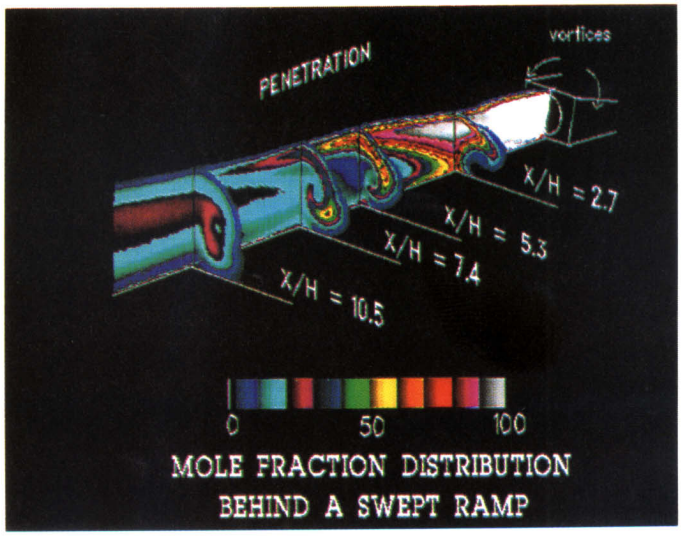

Fig. 9 Three-dimensional pictorial of the injectant plume for the Mach 2.9 flowfield.

dramatically distorted by the vortices than it was at this location in the Mach 2 flowfield. The same is true of the distribution at 3.19 ramp heights and of the distribution at 4.25 ramp heights. At these two locations, a thin stem of relatively high injectant mole fraction connects the injectant plume to the injector wall. For this reason, an inference of the injectant mole fraction in the region near the wall from the centerline distribution alone would be quite misleading. This fact vividly illustrates the need for spatially complete measurements in the crossflow planes for this geometry. At 5.31 ramp heights, the bulk of the injectant plume has been separated into a band similar to that in the Mach 2 flowfield and a small band along the top wall. The low injectant mole fraction core at this location corresponds to the isolated low mole fraction region in the centerline mole fraction distribution displayed in Fig. 7. At 6.38 ramp heights the injectant mole fraction in the center of the plume has begun to increase. The injectant mole fraction contours in the injectant plume are very close together, indicating that the vortex structure generated by the ramp at Mach 2.9 is much stronger than that generated at Mach 2. The vortex structure is still quite evident at 8.5 ramp heights, but at 10.63 ramp heights the influence of the discrete vortex structure is beginning to disappear. Finally, at 12.75 ramp heights, the influence of the coherent vortex structure on the mixing process appears to be nearly complete. At this location, the injectant mole fraction is everywhere less than stoichiometric but is greater than the injectant mole fraction at this location for the Mach 2 flowfield.

To illustrate the role of the streamwise vorticity in the mixing process, a three-dimensional representation of the injectant plume for the Mach 2.9 flowfield is included in Fig. 9. This pictorial was created from four of the crossflow injectant mole fraction distributions and the centerline distribution. From this pictorial, it can be seen that excellent agreement of the centerline mole fraction profiles exists between the penetration distribution and the crossflow distributions.

The planar mole fraction measurements, particularly the measurements in the crossflow planes, contain an enormous

amount of data which dramatically illustrates the mixing process. For CFD validations, statistical comparisons between the data and calculations can make use of all of the data[16]; however, to study mixing mechanisms and to compare various test section configurations and flow conditions, it is useful to represent the data in a more compact form. A variety of parameters may be employed in the study of mixing efficiencies. The two parameters represented in this study are the mixing rate, defined as the maximum injectant mole fraction at a given streamwise location, and the mixed area of the combustor, defined so that it can be calculated solely from the injectant mole fraction. For this work, the percent of the duct area which is mixed to within the static flammability limits, 4–75% hydrogen in the hydrogen-air mixture, is defined to be the mixed area. Figure 10 is a plot of the mixed area for the swept ramp injector at Mach 2 and 2.9. The mixed areas are essentially the same for the first two ramp heights but downstream of this point the mixed area is significantly higher at Mach 2 than at Mach 2.9. It appears that a maximum mixed area of approximately 20% of the duct is achieved at the X/H location at which the influence of the coherent vortex structure begins to disappear for both Mach 2 and 2.9. Although the vortex structure is apparently much stronger at Mach 2.9, this structure is stretched out in the streamwise direction and a longer length is required for the vortex structure to mix the injectant. At Mach 2.9, the mixed area increases strongly in the first six ramp heights of the mixing duct and then levels off abruptly. This duct location at which the mixed area levels off corresponds to the location at which the vortex structure begins to refill the core of the plume with significant amounts of injectant.

The mixing rate for the swept ramp injector at Mach 2 and 2.9 is plotted in Fig. 11. The mixing rate has been used extensively in the study of supersonic mixing and it has been shown that, for many injector geometries, the maximum mole fraction far downstream of the injectors is proportional to the distance from the injector raised to a constant power.[17] This proportionality has been used successfully to correlate the downstream mixing characteristics of a variety of supersonic mixing flows.[18] Figure 12 shows the mixing rate data for the

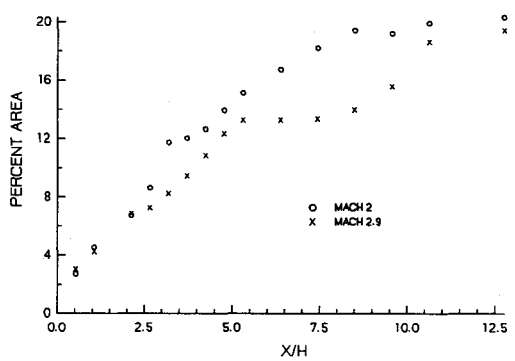

Fig. 10 Mixed area for swept ramp injector.

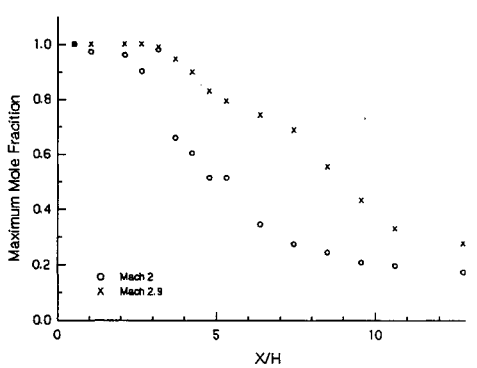

Fig. 11 Mixing rate for swept ramp injector.

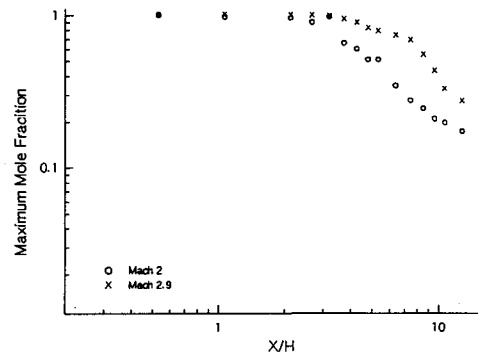

Fig. 12 Mixing rate for swept ramp injector: log-log plot.

ramped injector flowfields plotted on a log-log scale. While a small linear region exists for the Mach 2 flow field from X/H of about 2 to 8, no such region is apparent for the Mach 2.9 case. The mixing rate curve for Mach 2.9 suggests that the strong effects of the large scale streamwise vorticity in the region of the plume investigated in this work prevent the application of such a simple empirical relationship as that given in Ref. 17 in the portion of the flowfield investigated herein. It is clear from these mixing rate curves that the swept ramp injector mixes much faster at Mach 2 than at Mach 2.9. For example, at $X/H = 7$, the maximum mole fraction is approximately twice as high at Mach 2.9 as at Mach 2. Near the end of the test section, the maximum mole fraction has decreased to less than 25% for both Mach numbers; however, the Mach 2 flowfield has a lower maximum mole fraction and a correspondingly higher mixed area.

Concluding Remarks

An experimental investigation of vortex-enhanced mixing in a nonreacting supersonic combustor using near-parallel injection from the base of a swept ramp has been conducted. Shadowgraphs and fluorescence visualization photographs provide insight into the nature of the overall flowfield structure. Injectant mole fraction measurements at both Mach 2 and 2.9 quantitatively exhibit the mixing of the swept ramp injector and vividly demonstrate the effects of the ramp-generated vorticity on the injectant plume.

The following observations were made from these measurements. The supersonic injector core is initially turned toward the injector wall, but downstream of the Mach disk the injectant plume is dramatically distorted and lifted away from the injector wall by the ramp-generated vortices. These vortices mix freestream fluid into the center of the injectant plume, thereby enhancing the mixing of the injectant. These features are highly desirable for a hyper-mixing geometry in a SCRAMJET combustor. The second observation is that the domination of the injectant distribution in the plume by the large-scale, coherent, ramp-generated vortices appears to largely disappear at approximately 10 ramp heights downstream of the ramp base for both Mach 2 and 2.9. A third observation is that the effect of shocks on the injectant mole fraction distribution is slight, causing only a small turning of the plume. Finally, under conditions of constant equivalence ratio, as the freestream Mach number is increased from 2 to 2.9, the strength of the ramp-generated vortices is increased; however, the length of the vortex structure is increased, resulting in a decreased mixing rate at the higher Mach number.

Complete measured distributions of injectant mole fraction, such as those presented herein, provide the means for directly evaluating mixing efficiency and for comparing the mixing rates of various injector geometries and flowfield conditions. This injectant mole fraction measurement technique will be invaluable in evaluating injector geometries chosen for future hypermixing SCRAMJET combustors and in providing extensive data bases for the validation of computational fluid dynamic codes.

Acknowledgments

This work has been supported by the NASA Langley Research Center under Grant NAG-1-795, G. Burton Northam, technical monitor.

References

[1]Tillman, T. G., Patrick, W. P., and Paterson, R. W., "Enhanced Mixing of Supersonic Jets," AIAA/ASME/SAE/ASEE Twenty-Fourth Joint Propulsion Conf., AIAA Paper 88-3002, Boston, MA, July 1988.

[2]Northam, G. B., Greenberg, I., and Byington, C. S., "Evaluation of Parallel Injector Configurations for Supersonic Combustion," AIAA/ASME/SAE/ASEE Twenty-Fifth Joint Propulsion Conf., AIAA Paper 89-2525, Monterey, CA, July 1989.

[3]Drummond, J. P., Carpenter, M. H., Riggins, D. W., and Adams M. S., "Mixing Enhancement in a Supersonic Combustor," AIAA/ASME/SAE/ASEE Twenty-Fifth Joint Propulsion Conf., AIAA Paper 89-2794, Monterey, CA, July 1989.

[4]Riggins, D. W., Mekkes, G. L., McClinton, C.R., and Drummond, J. P., "A Numerical Study of Mixing Enhancement in a Supersonic Combustor," AIAA Twenty-Eighth Aerospace Sciences Meeting, AIAA Paper 90-0203, Reno, NV, Jan. 1990.

[5]McDaniel, J. C., and Graves, J., Jr., "Laser-Induced Fluorescence Visualization of Transverse Gaseous Injection in a Nonreacting Supersonic Combustor," *Journal of Propulsion and Power*, Vol. 4, No. 6, 1988, pp. 591–597.

[6]Whitehurst, R. B., Uenishi, K., McDaniel, J. C., and Northam, G. B., "Experimental and Numerical Studies of Transverse Fuel Injection Patterns in a Nonreacting Scramjet Combustor," AIAA/SAE/ASME/ASEE Twenty-Third Joint Propulsion Conf., AIAA Paper 87-2163, San Diego, CA, June–July 1987.

[7]Rapaganni, N. L., and Davis, S. L., "Laser-Induced Fluorescence: A Diagnostic for Fluid Mechanics," *Lasers and Applications*, May 1985, pp. 127–131.

[8]McDaniel, J. C., "Quantitative Measurement of Density and Velocity in Compressible Flows Using Laser-Induced Iodine Fluorescence," AIAA Twenty-First Aerospace Sciences Meeting, AIAA Paper 83-0049, Reno, NV, Jan. 1983.

[9]Hiller, B. H., and Hanson, R. K., "Simultaneous Planar Measurements of Velocity and Pressure Fields in Gas Flows Using Laser-Induced Fluorescence," *Applied Optics*, Vol. 27, No. 1, 1988, pp. 33–48.

[10]Hartfield, R. J., Jr., Hollo, S. D., and McDaniel, J. C., "Planar Temperature Measurement in Compressible Flows Using Laser-Induced Iodine Fluorescence," *Optics Letters*, Jan. 15, 1991, pp. 106–108.

[11]Ni-Imi, T., Fujimoto, and Shimizu, N., "Method for Planar Measurement of Temperature in Compressible Flow Using Two-Line Laser-Induced Iodine Fluorescence," *Optics Letters*, Vol. 15, No. 16, 1990, pp. 918–920.

[12]Hartfield, R. J., Jr., Abbitt, J. D., III, and McDaniel, J. C., "Injectant Mole Fraction Imaging in Compressible Mixing Flows Using Planar Laser-Induced Iodine Fluorescence," *Optics Letters*, Aug. 15, 1989, pp. 850–852.

[13]Hartfield, R. J., Hollo, S. D., and McDaniel, J. C., "A Unified Planar Measurement Technique for Compressible Flows Using Laser-Induced Iodine Fluorescence," AIAA Thirtieth Aerospace Sciences Meeting, AIAA Paper 92-0141, Reno, NV, Jan. 1992; see also *AIAA Journal*, Vol. 31, No. 3, 1993, pp. 483–490.

[14]Abbitt, J. D., Hartfield, R. J., and McDaniel, J. C., "Mole Fraction Imaging of Transverse Injection in a Ducted Supersonic Flow," *AIAA Journal*, Vol. 29, No. 3, 1991, pp. 431–435.

[15]Hollo, S. H., Hartfield, R. J., Jr., and McDaniel, J. C., "Injectant Mole Fraction Measurements of Transverse Injection in Constant Area Ducts," Twenty-First Plasmadynamics and Lasers Conf., AIAA Paper 90-1632, Seattle, WA, June 1990.

[16]Eklund, D. R., Northam, G. B., and Hartfield, R. J., "A Detailed Investigation of Staged Normal Injection into a Mach 2 Flow," Twenty-Seventh JANNAF Combustion Meeting, F. E. Warren AFB, Cheyenne, WY, Nov. 1990.

[17]Thomas, R. H., Schetz, J. A., and Billings, F. S., "Gaseous Injection in High Speed Flow," Ninth International Symposium on Air Breathing Engines, Athens, Greece, Sept. 1989.

[18]Hollo, S. D., McDaniel, J. C., and Hartfield, R. J., Jr., "Characterization of Supersonic Mixing in a Nonreacting Mach 2 Combustor," AIAA Thirtieth Aerospace Sciences Meeting, AIAA Paper 92-0093, Reno, NV, Jan. 1992; see also *AIAA Journal* (to be published).